Redox Biology 26 (2019) 101308

Contents lists available at ScienceDirect

Redox Biology

journal homepage: www.elsevier.com/locate/redox

Using MRI to measure *in vivo* free radical production and perfusion dynamics in a mouse model of elevated oxidative stress and neurogenic atrophy

Bumsoo Ahn[a], Nataliya Smith[b], Debra Saunders[b], Rojina Ranjit[a], Parker Kneis[a], Rheal A. Towner[b,c,f], Holly Van Remmen[a,d,e,f,*]

[a] *Aging & Metabolism Research Program, Oklahoma Medical Research Foundation, Oklahoma City, OK, USA*
[b] *Advanced Magnetic Resonance Center, Oklahoma Medical Research Foundation, Oklahoma City, OK, USA*
[c] *Department of Pathology and Pharmaceutical Sciences, OUHSC, Oklahoma City, OK, USA*
[d] *Department of Physiology, OUHSC, Oklahoma City, OK, USA*
[e] *Oklahoma City VA Medical Center, Oklahoma City, OK, USA*
[f] *Oklahoma Nathan Shock Center for Aging, Oklahoma City, OK, USA*

A B S T R A C T

Mitochondrial dysfunction, reactive oxygen species (ROS) and oxidative damage have been implicated to play a causative role in age-related skeletal muscle atrophy and weakness (i.e. sarcopenia). Mice lacking the superoxide scavenger CuZnSOD (*Sod1*$^{-/-}$) exhibit high levels of oxygen-derived radicals and oxidative damage, associated with neuronal and muscular phenotypes consistent with sarcopenia. We used magnetic resonance imaging (MRI) technology combined with immunospin-trapping (IST) to measure *in vivo* free radical levels in skeletal muscle from wildtype, *Sod1*$^{-/-}$ and *SynTgSod1*$^{-/-}$ mice, a mouse model generated using targeted expression of the human *Sod1* transgene specifically in neuronal tissues to determine the impact of motor neuron degeneration in muscle atrophy. By combining the spin trap DMPO (5,5-dimethyl-1-pyrroline *N*-oxide) and molecular MRI (mMRI), we monitored the level of free radicals in mouse hindlimb muscle. The level of membrane-bound macromolecular radicals in the quadriceps muscle was elevated by ~3-fold in *Sod1*$^{-/-}$ mice, but normalized to wildtype levels in *SynTgSod1*$^{-/-}$ rescue mice. Skeletal muscle mass was reduced by ~25–30% in *Sod1*$^{-/-}$ mice, but fully reversed in muscle from *SynTgSod1*$^{-/-}$ mice. Using perfusion MRI we also measured the dynamics of blood flow within mouse hindlimb. Relative muscle blood flow in *Sod1*$^{-/-}$ is decreased to ~50% of wildtype and remained low in the *SynTgSod1*$^{-/-}$ mice. Our findings are significant in that we have shown for the first time that *in vivo* free radical production in skeletal muscle is directly correlated to muscle atrophy in an experimental model of oxidative stress. Neuron-specific expression of CuZnSOD reverses the *in vivo* free radical production in skeletal muscle in the *Sod1*$^{-/-}$ mouse model and prevents muscle atrophy. These results further support the feasibility of using *in vivo* assessments of redox status in the progression of a pathological process such as sarcopenia. This approach can also be valuable for evaluating responses to pharmacologic interventions.

1. Introduction

Sarcopenia, the age-related loss of muscle mass and function, is the major contributor to frailty in the elderly and predisposes the aging population to injuries and morbidities. Although the molecular mechanisms underlying sarcopenia are not completely defined, excess reactive oxygen species (ROS) from mitochondria (mtROS) and resultant oxidative modifications are known to be associated with loss of muscle mass (i.e. atrophy) and contractile function [1,2]. For example, exercise training is an established intervention that can mitigate the effects of sarcopenia by up-regulating endogenous antioxidant enzymes in skeletal muscle and blood [3–6], supporting the importance of oxidative stress in the pathogenesis of sarcopenia. Despite the probable role of oxidative stress and redox imbalance in sarcopenia, isolating the specific role of oxidative stress *in vivo* in sarcopenia is challenging because of hormonal, nutritional, behavioral (i.e. inactivity), and physiological (i.e. inflammation) changes that occur during aging [7–11]. Our laboratory has established a redox dependent sarcopenia model, i.e., *Sod1*$^{-/-}$ mice lacking the cytoplasmic superoxide anion scavenger superoxide dismutase 1 (CuZnSOD). *Sod1*$^{-/-}$ mice exhibit high levels of oxidative stress, mitochondrial dysfunction and oxidative damage associated with impairment of neuromuscular junction (NMJ), mimicking underlying causes of sarcopenia in humans [7,12–15] and other mammals [1,16–18]. These mice show significant loss of muscle mass beginning in early adulthood yet they do not exhibit significant behavioral or other physiological alterations that affect skeletal muscle health, including inactivity, decreases in food consumption, or hormonal changes [1,16].

We have previously addressed the significance of presynaptic oxidative stress on sarcopenia using a neuronal rescue mouse model with

* Corresponding author. Oklahoma Medical Research Foundation, Aging & Metabolism Program, 825 NE 13th St, Oklahoma City, OK, 73104, USA.
E-mail address: Holly-VanRemmen@omrf.org (H. Van Remmen).

https://doi.org/10.1016/j.redox.2019.101308
Received 8 July 2019; Received in revised form 19 August 2019; Accepted 21 August 2019
Available online 21 August 2019

selective expression of human *Sod1* gene in neurons driven by a *Synapsin 1* promotor on the background of *Sod1*$^{-/-}$ mice (*SynTgSod1*$^{-/-}$) [18]. We have reported that these mice are fully protected against the early onset of neurogenic atrophy that occurs in *Sod1*$^{-/-}$ [18], demonstrating the significance of neuronal oxidative stress and deficit on skeletal muscle atrophy. The goal of the present study was to utilize MRI to measure free radical production *in vivo* in *Sod1*$^{-/-}$ mice, a model of increased muscle mass due to increased oxidative stress (*Sod1*$^{-/-}$ mice) and in a second model lacking *Sod1* in muscle but not in neurons that does not show atrophy. This comparison will allow us to determine whether the MRI results are consistent with the contrasting atrophy phenotypes we have previously established in these two models.

In vivo free radicals have previously been measured using electron paramagnetic resonance (EPR) spectroscopy coupled with spin trapping [19,20]. A limitation of this approach is that the spin adducts are short-lived due to reductive and oxidative properties in biological systems [21]. Here we used a molecular probe conjugated with an antibody that detects a spin trap DMPO (5,5-dimethyl-1-pyrroline *N*-oxide), and gadolinium (MRI contrast agent) as previously reported in other tissues [22–24]. We combined immuno-spin trapping (IST) with magnetic resonance imaging (MRI) to determine membrane-bound macromolecular free radicals in skeletal muscle. We used established animal models of oxidative stress using redox-disturbed (*Sod1*$^{-/-}$) [1,25–27] and rescue mice by neuron-specific Sod1 expression (*SynTgSod1*$^{-/-}$) [18]. This innovative approach allows us not only *in vivo* assessments of redox status, but also time-course measurements of these parameters during a disease progression (i.e. sarcopenia) or a pharmacological intervention.

2. Methods

2.1. Generation of SynTgSod1$^{-/-}$ from Sod1$^{-/-}$ mouse model

Sod1$^{-/-}$ mice were generated as previously described [28]. We previously established that the *Sod1*$^{-/-}$ mice exhibit a redox-dependent sarcopenia characterized by atrophy, contractile dysfunction, mitochondrial ROS, and neuromuscular disruption [1,17,25], which are typical phenotypes of sarcopenia in humans [12,14,29]. To evaluate the significance of neuronal oxidative stress in a sarcopenia process, we created mice expressing human *Sod1* gene specifically in neurons using *Synapsin 1* promotor as previously described and characterized [18,30]. We have demonstrated the neuron-specific CuZnSOD expression in the SynTg *Sod1*$^{-/-}$ mice [30].

2.2. Animals

Sod1$^{-/-}$, *Syn*Tg*Sod1*$^{-/-}$ and wildtype mice were housed in pathogen-free conditions and provided with water and food *ad libitum*. Adult (8–11 months old) male mice were used for this study. The Institutional Animal Care and Use Committee at Oklahoma Medical Research Foundation approved all procedures.

2.3. CuZnSOD and MnSOD activity

To confirm the genotypes of the animals, the activities of CuZnSOD and MnSOD were determined using a method previously described [31]. Briefly, we homogenized ~10–20 mg of frozen tissue using a buffer, containing 20 mM Tris, 0.05% Triton X, and protease inhibitor. We spun the homogenate at 14,000 rpm for 10 min and removed supernatant. Extracts containing a portion of tissues were separated on a 10% native gel (150 V in cold room for 2.5 h). Each gel was soaked in a solution containing nitroblue tetrazolium (NBT), riboflavin, and TEMED.

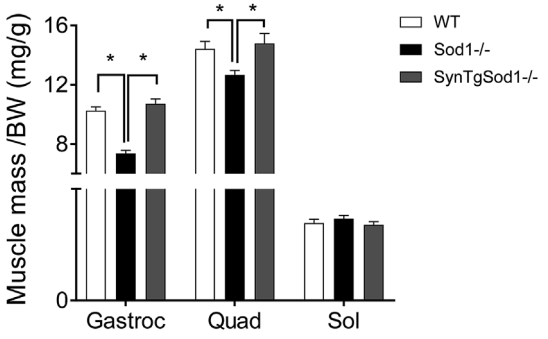

Fig. 1. Mice lacking CuZn Superoxide Dismutase (*Sod1*$^{-/-}$) exhibit an early onset of loss of muscle mass, while neuron specific expression of human SOD1 gene fully protects against atrophy in *Sod1*$^{-/-}$. Skeletal muscle mass normalized by body weight (mg/g). BW, body weight. n = 5–7. *$p < 0.05$. Gastroc, gastrocnemius; Quad, quadriceps; Sol, soleus.

2.4. Creation of MRI contrast agent specific to DMPO-radical adducts

The contrast agent, biotin-BSA (bovine serum albumin)-Gd (gadolinium)-DTPA, was prepared as previously described by our group [24], based on the modification of the method developed by Dafni et al. [32]. Anti-DMPO Ab (rabbit anti-mouse polyclonal) (Fig. 2C) was conjugated to the albumin moiety through a sulfo–NHS–EDC link (Fig. 2D) based on previous publications from the Towner laboratory [22,24].

2.5. DMPO and mMRI probe administration

We administered DMPO (ALX-430-090-G001, Enzo Life Sciences) i.p. (20 μg diluted in 200 μL of saline) 3 times daily (every 6 h) for 3 days to trap free radicals. Anti-DMPO probe was administered via tail vein during MRI experiments (Fig. 2E).

2.6. Magnetic resonance imaging

Morphological imaging: Mice were anesthetized and positioned in a stereotaxic cradle. A 30-cm horizontal bore Bruker Biospin magnet operating at 7 T (T; Bruker BioSpin GmbH, Karlsruhe, Germany), was used with a B-GA12SHP gradient set to perform all MRI experiments. Mice thighs were detected using a 40 mm quadrature volume coil. Multiple-slice RARE (rapid acquisition with relaxation enhancement) imaging (FOV = 3.0 × 3.0 cm^2, TR = 2500 ms, TE = 35 ms, matrix = 256 x 256, averages = 4, slices = 16, slice thickness = 1 mm) was used to obtain multiple thigh muscle images.

mMRI imaging: Molecular MRI was performed on mouse thigh muscles. The anti-DMPO probe with a biotin-albumin-Gd-DTPA construct bound to an anti-DMPO antibody was injected via a tail vein catheter in mice. A variable-TR RARE sequence (rapid acquisition with refocused echoes), with multiple TRs of 200, 400, 800, 1500, 3000 and 5500 ms, TE of 8.5 ms, FOV of 7.2 × 4.0 cm^2, matrix size of 256 × 192 and a spatial resolution of 0.208 mm was used to obtain T_1-weighted images before and after administration of the probe. Contrast difference images were created from the pre- and (90 min) post-contrast datasets for the slice of interest, by computing the difference in T1 relaxation times between the post-contrast and the pre-contrast image on a pixel basis. From difference images ten regions of interest (ROI), of equal size (0.05 cm^2), were drawn within areas with the highest signal intensity post-probe administration in the thigh muscle region. T1 relaxation times and signal intensities were affected by the presence of the Gd-containing molecular imaging probe.

Perfusion imaging: In order to assess microvascular alterations associated with thigh muscle microvascularity, the perfusion imaging method, arterial spin labeling, was used as previously described [33]. Perfusion maps were obtained on a single axial slice of the thigh

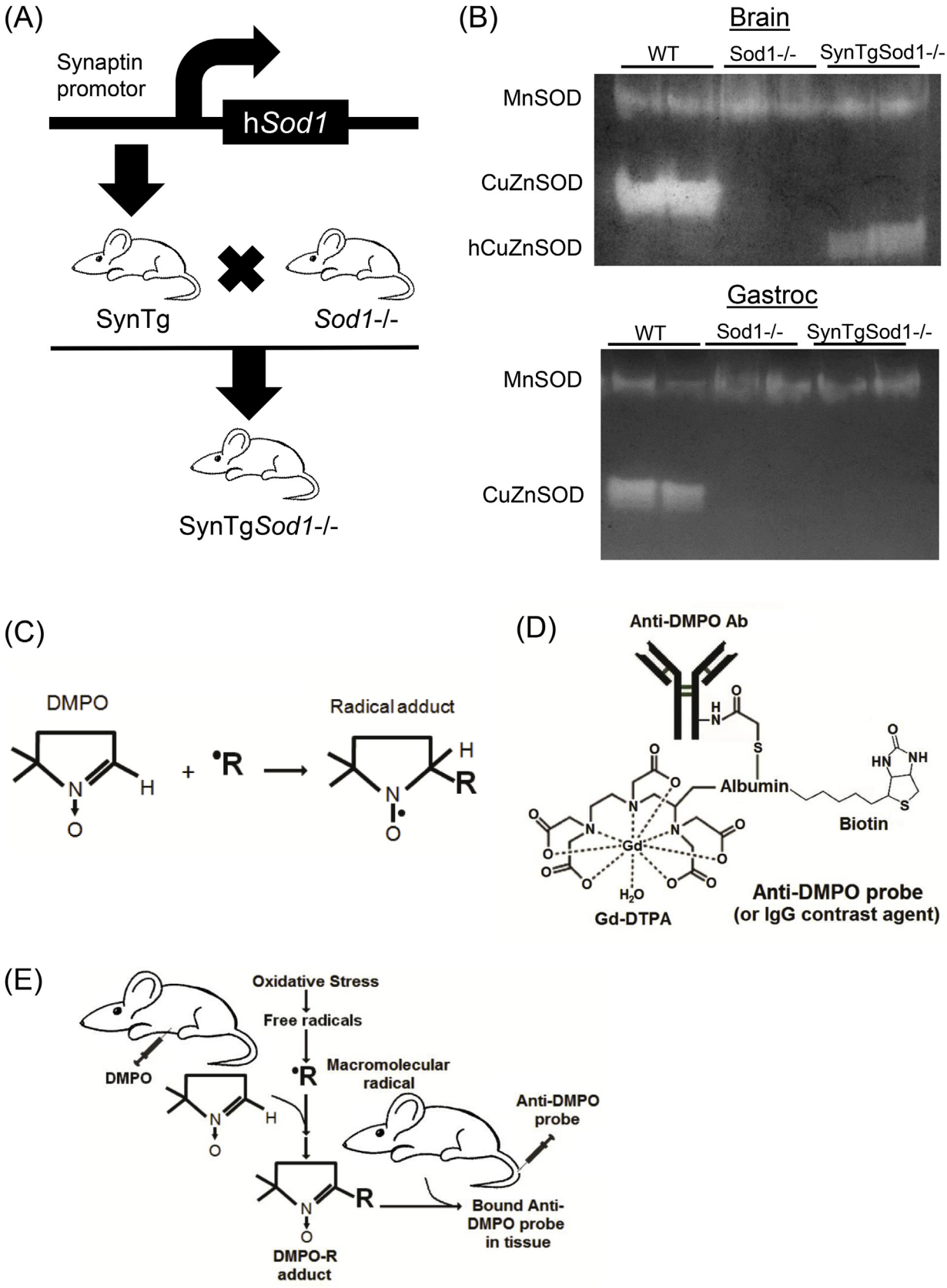

(caption on next page)

Fig. 2. Generation of neuron specific expression of *Sod1* in the *Sod1*$^{-/-}$ model (*SynTgSod1*$^{-/-}$), and a schematic representation of immunospin trap (IST) methodology to detect radical adducts in skeletal muscle. (A) SynTgSod1−/− mice were generated by crossing SynTG mice over expressing human Sod1 in neurons under the synapsin promoter and Sod1$^{-/-}$ mice in C57Bl6 genetic background. (B) Native gels stained for CuZnSOD and MnSOD enzyme activities from brain and gastrocnemius tissues. hCuZnSOD; human CuAnSOD. (C) A graphical representation of reaction by DMPO. A spin-trapping compound, 5,5-dimethyl-1-pyrroline N-oxide (DMPO), traps free radicals to form radical adducts (DMPO-R adducts). (D) DMPO adducts react with anti-DMPO probe conjugated with anti-DMPO antibody, gadolinium-DPTA, albumin, and biotin. (E) Combined immuno-spin trap (IST) and free radical-targeted mMRI approach. Initially, mice are administered DMPO (i.p.) to trap free radicals. Any cell membrane-bound radicals, including oxidized proteins and lipids can be detected by anti-DMPO probe, which is administered via a tail-vein catherter. Panels (C) to (E) are modified from Towner et al. [21]. i.p. intraperitoneal; mMRI, molecular magnetic resonance imaging.

muscle. The imaging geometry was a 3.5 × 3.5 mm^2 slice, of 1.5 mm in thickness, with a single shot echo-planar encoding over a 128 × 128 matrix. An echo time of 79 ms and a repetition time of 10 s were used. To obtain perfusion contrast, the flow alternating inversion recovery scheme was used, where inversion recovery images were acquired using selective and nonselective slices. For each type of inversion, 16 images were acquired with inversion times from 35 to 1600 ms. For perfusion data, the recovery curves obtained from each pixel for nonselective or selective inversion images were numerically fitted to derive pixel-wise T_1 and T_1* values, respectively, and longitudinal recovery rates were then used to calculate relative tissue blood flow, rTBF (mL/(100 g min)).

2.7. Statistical analyses

We performed 1-way ANOVA to compare means among genotypes followed by Tukey *post hoc* test (GraphPad 7.0 Software, San Diego, CA, USA). Data were means ± SEM. Statistical significance was set at $p < 0.05$.

3. Results

3.1. Redox-dependent atrophy in *Sod1*$^{-/-}$ is fully protected by neuron-specific *Sod1* expression. *Sod1*$^{-/-}$ mice exhibited ~30% loss of muscle mass in gastrocnemius, but the redox-dependent atrophy was fully protected by neuron-specific expression of *Sod1* (Fig. 1). This striking finding is consistent with our previous report [18]. The atrophy in gastrocnemius was also evident in another fast twitch-dominant muscle, quadriceps, but not present in soleus, consistent with previous observations in humans and animals [18]. We previously reported [1] that protein expression and activity of CuZnSOD is lacking in various tissues, including brain, liver and skeletal muscle and neuronal tissues in *Sod1*$^{-/-}$ mice. Crossing *Sod1*$^{-/-}$ with transgenic mice expressing h*Sod1* (Fig. 2A) increased protein expression and enzyme activity of CuZnSOD in brain [18] but not in skeletal muscle, confirming the targeted rescue of *Sod1* gene in neurons (Fig. 2B).

3.2. Membrane-bound macromolecular free radicals in *Sod1*$^{-/-}$ can be detected *in vivo* in skeletal muscle. Representative images of mMRI in mouse quadriceps muscles are shown in Fig. 3A. Anti-DMPO probe containing gadolinium demonstrates membrane-bound macromolecular radicals in T1-weighted (i) and contrast difference images (ii). Quantitative levels of macromolecular free radicals are ~3 fold elevated in *Sod1*$^{-/-}$, but the increase was abrogated by neuron-specific expression of *Sod1* (Fig. 3B). Our correlation analysis exhibits a significant relationship ($r = 0.74$, $p < 0.001$) between *in vivo* free radicals and atrophy in skeletal muscle for the first time (Fig. 3C).

3.3. Muscle blood flow *in vivo* is reduced in *Sod1*$^{-/-}$ and remained decreased in *SynTgSod1*$^{-/-}$. One of the underlying causes of aging that leads to sarcopenia is a reduced perfusion to skeletal muscle associated with oxidative stress [34,35]. Using arterial spin labeling MR images, we determined relative muscle blood flow (rMBF) in quadriceps muscle (Fig. 4A). Interestingly, the rMBF is decreased by ~50% in *Sod1*$^{-/-}$, and remained reduced in SynTg*Sod1*$^{-/-}$ (Fig. 4B), suggesting that neuron-specific expression of *Sod1* protects against atrophy independent of perfusion rate in muscle.

4. Discussion

Sarcopenia, the age-associated loss of skeletal muscle mass and function, has significant implications on the quality of life and health span in the elderly. Despite growing evidence supporting the significance of oxidative stress in sarcopenia, previous attempts to assess *in*

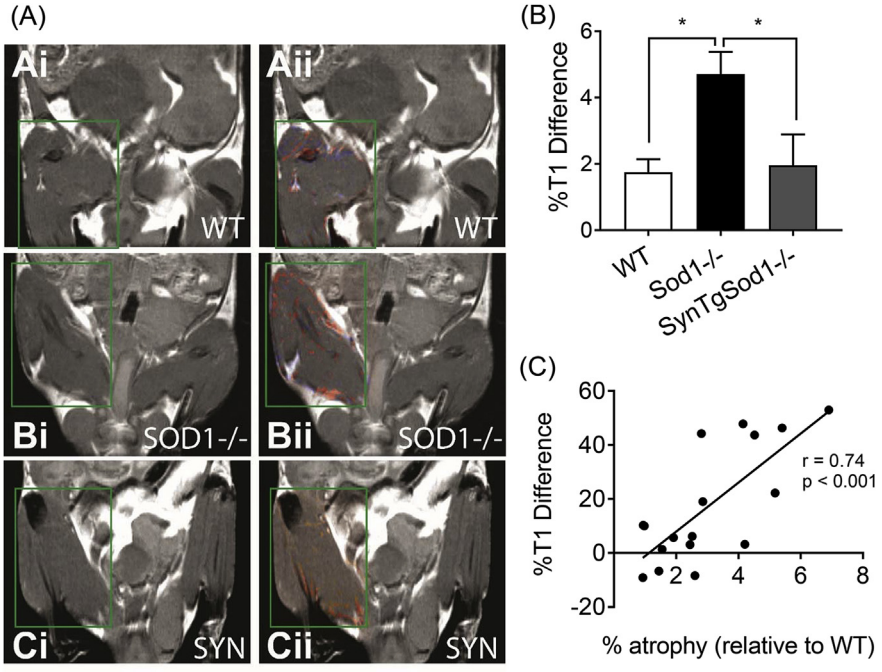

Fig. 3. A combination of molecular MRI and immunospin trap (IST) allows a real-time assessment of *in vivo* free radicals in mouse skeletal muscle. (A) Membrane-bound macromolecular free radicals from wildtype (WT), SOD1−/−, *SynTgSod1*$^{-/-}$ (SYN) in mouse thigh muscles. (i) T1-w MR images. (ii) Contrast difference images following administration of anti-DMPO probe which detects macromolecular free radicals. (B) Quantitative levels of macromolecular free radicals measured as percent (%) T1 differences associated with the presence of the anti-DMPO probe for WT, SOD1−/−, and SYN mice. (C) A relationship between percent atrophy against %T1 difference. n = 5–6. *$p < 0.05$.

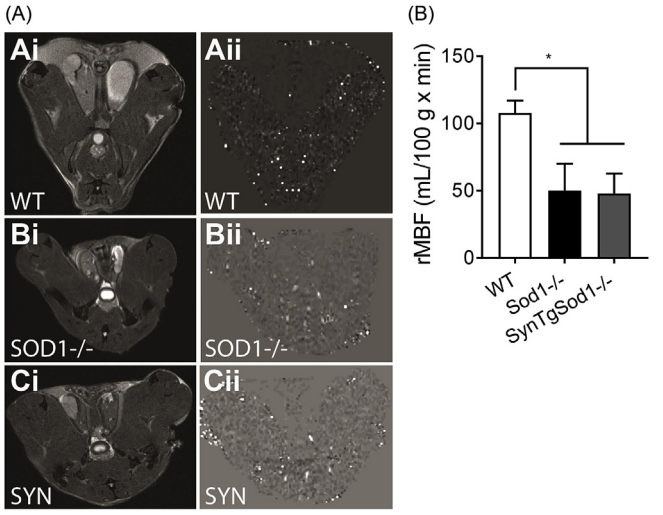

Fig. 4. Detection of *in vivo* changes in skeletal muscle blood flow. (A) Representative images of perfusion MRI from wildtype (WT), *Sod1*$^{-/-}$, *SynTgSod1*$^{-/-}$ (SYN). (i) T2-w MR images. (ii) Perfusion maps which demonstrate relative muscle blood flow (rMBF). (B) Quantified values of rMBF (mL/100 g x min) for WT, *Sod1*$^{-/-}$, and *SynTgSod1*$^{-/-}$ (SYN) mice. n = 5–6. *$p < 0.05$.

vivo free radicals were conducted by EPR coupled with spin trapping [19,20,36]. The disadvantage of the EPR approach is that the spin adducts (spin trapping agent-free radical adducts or aminoxyls) have short half-lives due to reductive and oxidative processes in biological systems [37]. Here, we demonstrate the feasibility of redox assessment *in vivo* by combining immunospin traping (IST) and molecular MRI (mMRI) that can significantly enhance the half-life of the free radicals in skeletal muscle. We used mouse skeletal hindlimb muscle and models of redox-dependent sarcopenia and rescue mice, *Sod1*$^{-/-}$ and *SynTgSod1*$^{-/-}$, to test the feasibility [1,17].

Spin trapping involves an addition of a diamagnetic molecule, usually a nitrone or nitroso compound, which reacts with free radicals (i.e. superoxide and hydroxyl free radicals) to give a stable paramagnetic spin adduct that accumulates and becomes observable by EPR. The limitation of the EPR spin trapping is that the spin adducts are short-lived. IST was developed using an antibody that recognizes macromolecular DMPO spin adducts, regardless of the redox status of the trapped radical adducts. The molecular probe (Fig. 2D) containing anti-DMPO antibody is conjugated with a gadolinium-based MRI contrast agent, which modifies relaxation times of nuclei. This approach has previously been used to assess redox status in several tissues other than skeletal muscle insulted by multiple pathologies, including glioblastoma, amyotrophic lateral sclerosis, and diabetes [22–24,38]. The construct also contains albumin for its wide distribution through circulation, as well as biotin for ex vivo histological confirmation.

We tested whether redox imbalance in skeletal muscle can be assessed *in vivo* using an established model of excess cytoplasmic superoxide that causes neurogenic atrophy (*Sod1*$^{-/-}$). We previously demonstrated that markers of oxidative stress are elevated in skeletal muscle, including lipid peroxidation, protein carbonylation, DNA damages, and oxidation of reducing agents (i.e. NAD/NADH) [18]. Consistent with our previous reports, we demonstrate here that the level of free radical production *in vivo* is increased by 3-fold in *Sod1*$^{-/-}$ mice using an IST-mMRI approach. The signals from mMRI are most likely membrane-bound macromolecular radicals. Since soluble DMPO adducts are likely to be metabolized and excreted through circulation, radicals bound to proteins and lipids residing in the membrane are primarily trapped by DMPO and detected by mMRI in tissues.

NMJ impairment has been reported in aged skeletal muscle from humans and rodents and is thought to be a causal factor in sarcopenia. In a previous study to test the causality of neuronal oxidative stress on sarcopenia, we replaced CuZnSOD in the neurons of the *Sod1*$^{-/-}$ mice using a neuron specific human *Sod1* transgene to protect neurons from oxidative stress. Surprisingly this intervention completely reversed the sarcopenia phenotype in the *Sod1*$^{-/-}$ mice. The atrophy that occurs in gastrocnemius and quadriceps of *Sod1*$^{-/-}$ mice was absent in the rescue transgenic mice (Fig. 1), consistent with our previous report [18]. Interestingly, the atrophy was only apparent in gastrocnemius and quadriceps muscles but not in soleus, consistent with our previous report [18]. Soleus is a slow-twitch dominant and anti-gravity muscle continuously recruited for locomotor activities. Increased activity level or the mitochondrial contents might provide protections against atrophy. We demonstrate that the increases in membrane bound radicals are restored by neuronal expression of *Sod1*. Further, the *in vivo* free radical levels are moderately correlated (r = 0.74) with atrophy, consistent with previous findings [18].

One of the consequences with aging is a decline in muscle blood flow, which might contribute to oxygen deficit and reduced mitochondrial bioenergetics of aged skeletal muscle. The potential role of oxidative stress in this process has been demonstrated by antioxidant intervention studies that significantly improved skeletal muscle perfusion rate in young and old individuals [34]. Consistent with existing literature in humans, *Sod1*$^{-/-}$ and the rescue transgenic mice both exhibited a diminished muscle blood flow, potentially due to impaired nitric oxide-dependent vasodilation in vasculature. Our data suggest that the improved skeletal muscle mass (Fig. 1) and contractile function [18] in *SynTgSod1*$^{-/-}$ was independent of reduced perfusion. It is noteworthy that end-exercise perfusion rate is decreased in aged calf muscles, but the hypo-perfusion did not reduce muscle oxidative capacity compared with young subjects [39].

In summary, we have shown that free radical levels can be assessed by MRI technology coupled with IST in skeletal muscle in a mouse model of neurogenic atrophy. We showed an inverse relationship between muscle mass and *in vivo* free radicals in skeletal muscle for the first time. This innovative approach allows us not only *in vivo* assessments of redox status, but also time-course assessments of these parameters during a disease progression (i.e. sarcopenia) or a pharmacological intervention.

Acknowledgements

The authors would like to thank the Advanced Magnetic Resonance Center for sharing their expertise. This work was supported by Pilot Research Program from Oklahoma Nathan Shock Center, Irene Diamond Fund/AFAR Postdoctoral Transition Awards to Bumsoo Ahn, National Institutes of Health [R01 NS092458, S10 OD023508] to Rheal Towner, and the National Institute on Aging [P01 AG051442, R01 AG050676, P30 AG050911] and a Merit Review from the United States Department of Veterans Affairs to Holly Van Remmen. Dr. Van Remmen is also supported by a Senior Research Career Scientist award from the Department of Veterans Affairs.

References

[1] F.L. Muller, W. Song, Y. Liu, A. Chaudhuri, S. Pieke-Dahl, R. Strong, T.-T. Huang, C.J. Epstein, L.J. Roberts, M. Csete, J.A. Faulkner, H. Van Remmen, Absence of CuZn superoxide dismutase leads to elevated oxidative stress and acceleration of age-dependent skeletal muscle atrophy, Free Radic. Biol. Med. 40 (2006) 1993–2004, https://doi.org/10.1016/j.freeradbiomed.2006.01.036.

[2] F.L. Muller, W. Song, Y.C. Jang, Y. Liu, M. Sabia, A. Richardson, H. Van Remmen, Denervation-induced skeletal muscle atrophy is associated with increased mitochondrial ROS production, Am. J. Physiol. Regul. Integr. Comp. Physiol. 293 (2007) R1159–R1168, https://doi.org/10.1152/ajpregu.00767.2006.

[3] M.H. Laughlin, T. Simpson, W.L. Sexton, O.R. Brown, J.K. Smith, R.J. Korthuis, Skeletal muscle oxidative capacity, antioxidant enzymes, and exercise training, J. Appl. Physiol. 68 (1990) 2337–2343, https://doi.org/10.1152/jappl.1990.68.6.2337.

[4] A.B. Morton, A. Mor Huertas, J.M. Hinkley, N. Ichinoseki-Sekine, D.D. Christou, A.J. Smuder, Mitochondrial accumulation of doxorubicin in cardiac and diaphragm

muscle following exercise preconditioning, Mitochondrion (2018), https://doi.org/10.1016/j.mito.2018.02.005.
[5] M.M. Kanter, R.L. Hamlin, D.V. Unverferth, H.W. Davis, A.J. Merola, Effect of exercise training on antioxidant enzymes and cardiotoxicity of doxorubicin, J. Appl. Physiol. 59 (1985) 1298–1303, https://doi.org/10.1152/jappl.1985.59.4.1298.
[6] K. Azizbeigi, S.R. Stannard, S. Atashak, M. Mosalman Haghighi, Antioxidant enzymes and oxidative stress adaptation to exercise training: comparison of endurance, resistance, and concurrent training in untrained males, J. Exerc. Sci. Fit. 12 (2014) 1–6, https://doi.org/10.1016/j.jesf.2013.12.001.
[7] B.E. Tomlinson, D. Irving, The numbers of limb motor neurons in the human lumbosacral cord throughout life, J. Neurol. Sci. 34 (1977) 213–219.
[8] I.M. Chapman, Weight loss in older persons, Med. Clin. N. Am. 95 (2011) 579–593, https://doi.org/10.1016/j.mcna.2011.02.004 xi.
[9] C.M. Jankowski, P. Wolfe, S.J. Schmiege, K.S. Nair, S. Khosla, M. Jensen, D. von Muhlen, G.A. Laughlin, D. Kritz-Silverstein, J. Bergstrom, R. Bettencourt, E.P. Weiss, D.T. Villareal, W.M. Kohrt, Sex-specific effects of dehydroepiandrosterone (DHEA) on bone mineral density and body composition: a pooled analysis of four clinical trials, Clin. Endocrinol. (Oxf). 90 (2019) 293–300, https://doi.org/10.1111/cen.13901.
[10] F.J. Steyn, S.T. Ngo, V.P. Chen, L.C. Bailey-Downs, T.Y. Xie, M. Ghadami, S. Brimijoin, W.M. Freeman, M. Rubinstein, M.J. Low, M.B. Stout, 17α-estradiol acts through hypothalamic pro-opiomelanocortin expressing neurons to reduce feeding behavior, Aging Cell 17 (2018), https://doi.org/10.1111/acel.12703.
[11] J.F. Sallis, Age-related decline in physical activity: a synthesis of human and animal studies, Med. Sci. Sport. Exerc. 32 (2000) 1598–1600.
[12] J. Lexell, D.Y. Downham, The occurrence of fibre-type grouping in healthy human muscle: a quantitative study of cross-sections of whole vastus lateralis from men between 15 and 83 years, Acta Neuropathol. 81 (1991) 377–381.
[13] F.G. Jennekens, B.E. Tomlinson, J.N. Walton, Histochemical aspects of five limb muscles in old age. An autopsy study, J. Neurol. Sci. 14 (1971) 259–276.
[14] N.A. Kelly, K.G. Hammond, M.J. Stec, C.S. Bickel, S.T. Windham, S.C. Tuggle, M.M. Bamman, Quantification and Characterization of Grouped Type I Myofibers in Human Aging, Muscle Nerve vol. 57, (2018) E52–E59, https://doi.org/10.1002/mus.25711.
[15] M. Tomonaga, Histochemical and ultrastructural changes in senile human skeletal muscle, J. Am. Geriatr. Soc. 25 (1977) 125–131.
[16] Y.C. Jang, M.S. Lustgarten, Y. Liu, F.L. Muller, A. Bhattacharya, H. Liang, A.B. Salmon, S.V. Brooks, L. Larkin, C.R. Hayworth, A. Richardson, H. Van Remmen, Increased superoxide in vivo accelerates age-associated muscle atrophy through mitochondrial dysfunction and neuromuscular junction degeneration, FASEB J. 24 (2010) 1376–1390, https://doi.org/10.1096/fj.09-146308.
[17] Y.C. Jang, H. Van Remmen, Age-associated alterations of the neuromuscular junction, Exp. Gerontol. 46 (2011) 193–198, https://doi.org/10.1016/j.exger.2010.08.029.
[18] G.K. Sakellariou, C.S. Davis, Y. Shi, M.V. Ivannikov, Y. Zhang, A. Vasilaki, G.T. Macleod, A. Richardson, H. Van Remmen, M.J. Jackson, A. McArdle, S.V. Brooks, Neuron-specific expression of CuZnSOD prevents the loss of muscle mass and function that occurs in homozygous CuZnSOD-knockout mice, FASEB J. 28 (2014) 1666–1681, https://doi.org/10.1096/fj.13-240390.
[19] S.W. Flanagan, P.L. Moseley, G.R. Buettner, Increased flux of free radicals in cells subjected to hyperthermia: detection by electron paramagnetic resonance spin trapping, FEBS (Fed. Eur. Biochem. Soc.) Lett. 431 (1998) 285–286, https://doi.org/10.1016/S0014-5793(98)00779-0.
[20] N. KHAN, S.P. MUPPARAJU, D. MINTZOPOULOS, M. KESARWANI, V. RIGHI, L.G. RAHME, H.M. SWARTZ, A.A. TZIKA, Burn trauma in skeletal muscle results in oxidative stress as assessed by in vivo electron paramagnetic resonance, Mol. Med. Rep. 1 (2008) 813–819, https://doi.org/10.3892/mmr-00000033.
[21] R.A. Towner, N. Smith, Vivo and in situ detection of macromolecular free radicals using immuno-spin trapping and molecular magnetic resonance imaging, Antioxidants Redox Signal. 28 (2018) 1404–1415, https://doi.org/10.1089/ars.2017.7390.
[22] R.A. Towner, N. Smith, D. Saunders, M. Henderson, K. Downum, F. Lupu, R. Silasi-Mansat, D.C. Ramirez, S.E. Gomez-Mejiba, M.G. Bonini, M. Ehrenshaft, R.P. Mason, In vivo imaging of immuno-spin trapped radicals with molecular magnetic resonance imaging in a diabetic mouse model, Diabetes 61 (2012) 2405–2413, https://doi.org/10.2337/db11-1540.
[23] R.A. Towner, N. Smith, D. Saunders, F. Lupu, R. Silasi-Mansat, M. West, D.C. Ramirez, S.E. Gomez-Mejiba, M.G. Bonini, R.P. Mason, M. Ehrenshaft, K. Hensley, In vivo detection of free radicals using molecular MRI and immuno-spin trapping in a mouse model for amyotrophic lateral sclerosis, Free Radic. Biol. Med. 63 (2013) 351–360, https://doi.org/10.1016/j.freeradbiomed.2013.05.026.
[24] R.A. Towner, N. Smith, D. Saunders, C.A. Brown, X. Cai, J. Ziegler, S. Mallory, M.G. Dozmorov, P. Coutinho De Souza, G. Wiley, K. Kim, S. Kang, D.-S. Kong, Y.-T. Kim, K.-M. Fung, J.D. Wren, J. Battiste, OKN-007 increases temozolomide (TMZ) sensitivity and suppresses TMZ-resistant glioblastoma (GBM) tumor growth, Transl Oncol 12 (2019) 320–335, https://doi.org/10.1016/j.tranon.2018.10.002.
[25] Y. Shi, M.V. Ivannikov, M.E. Walsh, Y. Liu, Y. Zhang, C.A. Jaramillo, G.T. Macleod, H. Van Remmen, The lack of CuZnSOD leads to impaired neurotransmitter release, neuromuscular junction destabilization and reduced muscle strength in mice, PLoS One 9 (2014) e100834, , https://doi.org/10.1371/journal.pone.0100834.
[26] Y.C. Jang, Y. Liu, C.R. Hayworth, A. Bhattacharya, M.S. Lustgarten, F.L. Muller, A. Chaudhuri, W. Qi, Y. Li, J.-Y. Huang, E. Verdin, A. Richardson, H. Van Remmen, Dietary restriction attenuates age-associated muscle atrophy by lowering oxidative stress in mice even in complete absence of CuZnSOD, Aging Cell 11 (2012) 770–782, https://doi.org/10.1111/j.1474-9726.2012.00843.x.
[27] Y. Zhang, C. Davis, G.K. Sakellariou, Y. Shi, A.C. Kayani, D. Pulliam, A. Bhattacharya, A. Richardson, M.J. Jackson, A. McArdle, S.V. Brooks, H. Van Remmen, CuZnSOD gene deletion targeted to skeletal muscle leads to loss of contractile force but does not cause muscle atrophy in adult mice, FASEB J. 27 (2013) 3536–3548, https://doi.org/10.1096/fj.13-228130.
[28] T.T. Huang, M. Yasunami, E.J. Carlson, A.M. Gillespie, A.G. Reaume, E.K. Hoffman, P.H. Chan, R.W. Scott, C.J. Epstein, Superoxide-mediated cytotoxicity in superoxide dismutase-deficient fetal fibroblasts, Arch. Biochem. Biophys. 344 (1997) 424–432, https://doi.org/10.1006/abbi.1997.0237.
[29] J. Lexell, C.C. Taylor, M. Sjöström, What is the cause of the ageing atrophy? Total number, size and proportion of different fiber types studied in whole vastus lateralis muscle from 15- to 83-year-old men, J. Neurol. Sci. 84 (1988) 275–294.
[30] K. Sataranatarajan, R. Qaisar, C. Davis, G.K. Sakellariou, A. Vasilaki, Y. Zhang, Y. Liu, S. Bhaskaran, A. McArdle, M. Jackson, S.V. Brooks, A. Richardson, H. Van Remmen, Neuron specific reduction in CuZnSOD is not sufficient to initiate a full sarcopenia phenotype, Redox Biol 5 (2015) 140–148, https://doi.org/10.1016/j.redox.2015.04.005.
[31] H. Van Remmen, C. Salvador, H. Yang, T.T. Huang, C.J. Epstein, A. Richardson, Characterization of the antioxidant status of the heterozygous manganese superoxide dismutase knockout mouse, Arch. Biochem. Biophys. 363 (1999) 91–97, https://doi.org/10.1006/abbi.1998.1060.
[32] H. Dafni, L. Landsman, B. Schechter, F. Kohen, M. Neeman, MRI and fluorescence microscopy of the acute vascular response to VEGF165: vasodilation, hyper-permeability and lymphatic uptake, followed by rapid inactivation of the growth factor, NMR Biomed. 15 (2002) 120–131.
[33] R.A. Towner, D. Saunders, N. Smith, W. Towler, M. Cruz, S. Do, J.E. Maher, K. Whitaker, M. Lerner, K.A. Morton, Assessing long-term neuroinflammatory responses to encephalopathy using MRI approaches in a rat endotoxemia model, GeroScience 40 (2018) 49–60, https://doi.org/10.1007/s11357-018-0009-z.
[34] D.W. Wray, S.K. Nishiyama, A. Monnet, C. Wary, S.S. Duteil, P.G. Carlier, R.S. Richardson, Antioxidants and aging: NMR-based evidence of improved skeletal muscle perfusion and energetics, Am. J. Physiol. Heart Circ. Physiol. 297 (2009) H1870–H1875, https://doi.org/10.1152/ajpheart.00709.2009.
[35] R.D. Prisby, M.W. Ramsey, B.J. Behnke, J.M. Dominguez, A.J. Donato, M.R. Allen, M.D. Delp, Aging reduces skeletal blood flow, endothelium-dependent vasodilation, and NO bioavailability in rats, J. Bone Miner. Res. 22 (2007) 1280–1288, https://doi.org/10.1359/jbmr.070415.
[36] H. Eto, F. Hyodo, N. Kosem, R. Kobayashi, K. Yasukawa, M. Nakao, M. Kiniwa, H. Utsumi, Redox imaging of skeletal muscle using in vivo DNP-MRI and its application to an animal model of local inflammation, Free Radic. Biol. Med. 89 (2015) 1097–1104, https://doi.org/10.1016/j.freeradbiomed.2015.10.418.
[37] E.G. Janzen, [22] Spin trapping, Methods in Enzymology, Academic Press, 1984, pp. 188–198, , https://doi.org/10.1016/S0076-6879(84)05025-4.
[38] R.A. Towner, N. Smith, S. Doblas, Y. Tesiram, P. Garteiser, D. Saunders, R. Cranford, R. Silasi-Mansat, O. Herlea, L. Ivanciu, D. Wu, F. Lupu, In vivo detection of c-Met expression in a rat C6 glioma model, J. Cell Mol. Med. 12 (2008) 174–186, https://doi.org/10.1111/j.1582-4934.2008.00220.x.
[39] D.W. Wray, S.K. Nishiyama, A. Monnet, C. Wary, S. Duteil, P.G. Carlier, R.S. Richardson, Multiparametric NMR-based assessment of skeletal muscle perfusion and metabolism during exercise in elderly persons: preliminary findings, J Gerontol A Biol Sci Med Sci 64A (2009) 968–974, https://doi.org/10.1093/gerona/glp044.